sustainability

MDPI

Article

A Core-Shell Amino-Functionalized Magnetic Molecularly Imprinted Polymer Based on Glycidyl Methacrylate for Dispersive Solid-Phase Microextraction of Aniline

Tamara Tadić [1], Bojana Marković [1], Jelena Radulović [2], Jelena Lukić [3], Ljiljana Suručić [4], Aleksandra Nastasović [1] and Antonije Onjia [5,*]

[1] Institute of Chemistry, Technology and Metallurgy, University of Belgrade, Njegoševa 12, 11000 Belgrade, Serbia; tamara.tadic@ihtm.bg.ac.rs (T.T.); bojana.markovic@ihtm.bg.ac.rs (B.M.); aleksandra.nastasovic@ihtm.bg.ac.rs (A.N.)
[2] Anahem Laboratory, Mocartova 10, 11160 Belgrade, Serbia; radulovic.jelena@anahem.org
[3] Innovation Center of the Faculty of Technology and Metallurgy, Karnegijeva 4, 11000 Belgrade, Serbia; jlukic@tmf.bg.ac.rs
[4] Faculty of Medicine, University of Banja Luka, Save Mrkalja 14, 78000 Banja Luka, Bosnia and Herzegovina; ljiljana.surucic@med.unibl.org
[5] Faculty of Technology and Metallurgy, University of Belgrade, Karnegijeva 4, 11000 Belgrade, Serbia
* Correspondence: onjia@tmf.bg.ac.rs

Abstract: A core-shell amino-functionalized glycidyl methacrylate magnetic molecularly imprinted polymer (MIP) was synthesized by the suspension polymerization/surface imprinting method and characterized by Fourier transform infrared spectroscopy (FTIR), scanning electron microscopy (SEM), mercury porosimetry, nitrogen gas adsorption–desorption, and elemental analysis. This MIP was used as the sorbent in dispersive solid-phase microextraction (DSPME) of aniline from textile wastewater prior to high-performance liquid chromatography-mass spectrometry (HPLC-MS) measurements. Since aniline is toxic and a probable human carcinogen, its determination in water is of great significance. This is a challenging task because aniline is usually present at trace levels. The effects of different DSPME variables on the preconcentration efficiency have been studied by using the Plackett–Burman screening design of experiments (DoE) followed by response surface methodology optimization using the Box-Behnken design. Thus, DoE enabled the investigation of several variables simultaneously. Under optimized conditions, aniline was effectively and selectively separated by a small amount of the DSPME sorbent and detected in real textile wastewater samples. The method detection limit of 1 ng mL^{-1} was attained, with good method linearity and acceptable recovery and precision. The results showed that the studied MIP could be a reliable DSPME sorbent for efficiently analyzing trace aniline in real wastewater samples.

Keywords: DSPME; aromatic amines; wastewater; LC-MS/MS; MIP; design of experiment

Citation: Tadić, T.; Marković, B.; Radulović, J.; Lukić, J.; Suručić, L.; Nastasović, A.; Onjia, A. A Core-Shell Amino-Functionalized Magnetic Molecularly Imprinted Polymer Based on Glycidyl Methacrylate for Dispersive Solid-Phase Microextraction of Aniline. *Sustainability* **2022**, *14*, 9222. https://doi.org/10.3390/su14159222

Academic Editor: Salvatore Cataldo

Received: 16 June 2022
Accepted: 23 July 2022
Published: 27 July 2022

1. Introduction

The textile industry is a leading consumer of water (of about 100–200 L of water per kg of textile product), ranking in the top ten water-consuming industries [1]. On the other hand, textile industries generate large amounts of wastewater containing various toxic, carcinogenic, mutagenic, or teratogenic chemicals such as azo dyes [2]. The high concentration of toxic materials and pH, high salinity, and turbidity have a detrimental ecological impact and make the treatment of textile industry effluents highly problematic.

Aniline ($C_6H_5NH_2$), an organic compound in which the primary amino group is attached to an aromatic ring, represents one of the most important organic intermediates in textile industries, as well as in the production of drugs, polyurethanes, pesticides, rubber, plastics, varnishes, and pigments [3]. The primary exposure to aniline is through azo dyes used in the textile industry for dyeing textiles and leather [4]. Polluted wastewater could

affect river ecosystems and human health [5,6], as well as soils [7]. When aniline reaches the water, it inhibits the growth of aquatic plants and animals and thus directly or indirectly harms human health through the food chain [8]. According to the USA Environmental Protection Agency (EPA), aniline has been classified as a Group B2 (probable human carcinogen) and very toxic in humans, with a probable oral lethal dose in humans at 50–500 mg kg^{-1}·bw [9].

Determining aniline in real water samples is a challenge because of its trace level concentration. Therefore, adopting an appropriate sample preparation strategy is critical in increasing the sensitivity and accuracy of methods for aniline determination. Instrumental techniques, such as high-performance liquid chromatography (HPLC) and gas chromatography (GC), suffer from many limitations, such as relatively high detection limits and matrix interference. Due to these problems, sample purification and microextraction techniques can be used [10].

Dispersive solid-phase microextraction (DSPME) is a relatively new technique developed to improve the contact area between sorbent and sample solution, shorten the extraction time and decrease the sorbents consumption [11]. The advantage of DSPME is reflected in the use of highly efficient sorbents to improve the preconcentration of the analytes using only a few milligrams of sorbents [12]. Furthermore, due to its efficiency, magnetic molecularly imprinted polymers could be used as sorbents, which can be easily removed from the solution due to their magnetic properties [13].

Molecularly imprinted polymers (MIPs) are interesting sorbents in environmental research for analyzing target pollutants due to their size, larger surface area, selectivity, and reusability [14]. Molecular imprinting is used to form specific recognition sites in the polymer matrix, where pattern memory is achieved by shape recognition. A template molecule, which could be a target compound, its fragment, or a molecule similar in shape, size, or functional groups (dummy template), is added to the mixture to interact with the monomers [15]. After removing the template, binding sites are established that are complementary in shape, size, and functionality to the target molecule [16].

MIPs have found applications in various areas such as chemical sensors [17], dispersive solid-phase microextraction [18], chromatography separation [19], detection of human viral pathogens [20], wastewater treatment [21], etc. (Figure 1).

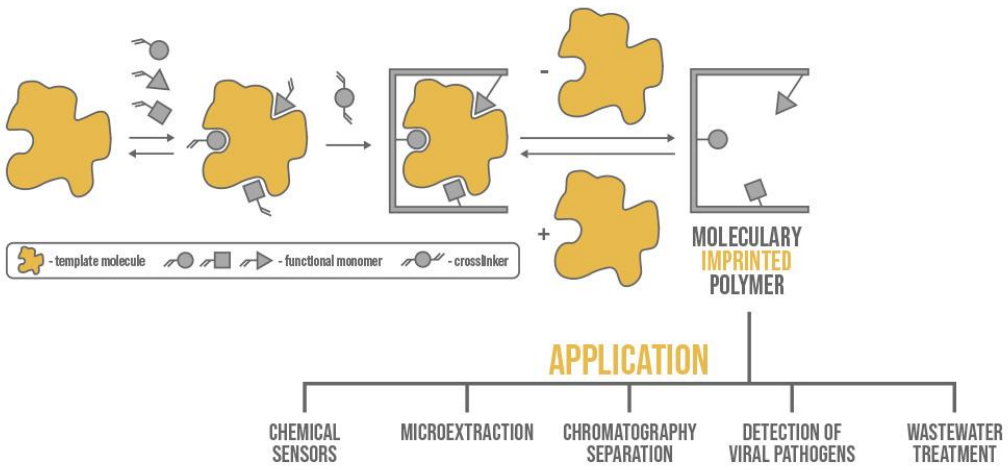

Figure 1. Introduction and application of MIP.

Due to their chemical stability and controlled morphology, modification in various ways allows porous materials to be applied to target analytes [22]. Commonly used functional monomers for molecular imprinting technique are methacrylic acid (MAA), 2- or 4-vinylpyridine (2- or 4-VP), acrylic acid (AA), acrylamide, and styrene, while commonly used cross-linkers are ethylene glycol dimethacrylate (EGDMA), trimethylolpropane trimethacrylate (TRIM), and divinylbenzene (DVB) [23].

Because of the presence of epoxy groups which offer numerous modification possibilities, polymers based on glycidyl methacrylate (GMA) have versatile applications, such as sorption of metals [24,25], textile dyes [26], and organic pollutants [27]. GMA is mostly used as co-monomer in the synthesis of MIPs [28,29], while MIP based on GMA as only monomer has not been developed for the removal of aniline so far. Epoxy ring from GMA enables successful amino-functionalization and preparation of MIP.

Magnetic nanocomposites are widely studied for use in water purification due to their ease of use and removal, non-toxicity, and cost-effectiveness [30]. The core-shell nanoparticles comprise magnetic nanoparticles as a center and external shell silica coating. This empowers better recuperation and separation by the magnet [31].

The research aims to develop an efficient, environmentally friendly polymer material that shows selectivity for aniline and a reliable microextraction technique of aniline from textile wastewater prior to instrumental measurement. MIP, which consists of a silanized Fe_3O_4 core and the amino-functionalized shell, was successfully synthesized by suspension polymerization and the surface imprinting technique. Due to the large number of variables that affect the DSPME technique, the Design of Experiment (DoE) was used to optimize the method. Thus, the Plackett–Burman design (PBD) was used for screening, and the Box–Behnken design (BBD) was used for optimization.

Advantages of this research are reflected in the use of a small amount of sorbent, easy removal, no need for centrifugation step for the sorbent separation, low analysis time, and conditions that do not require an additional investment of energy in the process, reduced number of experiments thanks to DoE. However, using of core-shell amino-functionalized MIP based on GMA as DSPME sorbent for aniline preconcentration optimized with DoE has not been studied yet.

2. Materials and Methods

2.1. Chemicals

All the chemicals used for MIP synthesis were of analytical-grade products and used as received. Glycidyl methacrylate (GMA), pentaethylenehexamine (PEHA), 2,2′-azobisisobutyronitrile (AIBN), cyclopentanol, and 1-tetradecanol were purchased from Merck KGaA (Darmstadt, Germany). Aniline (ReagentPlus, 99%), ethylene glycol dimethacrylate (EGDMA), tetraethyl orthosilicate (TEOS), 3-methacryloxypropyltrimethoxysilane (MPS), and magnetite (iron (II, III) oxide, nanopowder, <50 nm particle size (TEM), 98% trace metals basis), ammonium hydroxide (NH_3 solution, 25 wt.%) were obtained from Sigma-Aldrich Chemie GmbH (Taufkirchen, Germany). Poly(N-vinyl pyrrolidone) (PVP, Kollidone 90) was purchased from BASF SE (Ludwigshafen, Germany). Methanol and acetonitrile were obtained from Carlo Erba Reagents GmbH (Emmendingen, Germany), hydrochloric acid 35% was purchased from Lach-Ner s.r.o. (Brno, Czech Republic), and sodium hydroxide (p.a. > 98%) was obtained from Centrohem d.o.o. (Stara Pazova, Serbia). All solutions were prepared with deionized water. All the chemicals were of analytical grade.

2.2. Instrumentation

Fourier transform infrared (FTIR) spectra were taken in ATR mode using a Nicolet SUMMIT FT-IR Spectrometer (Thermo Fisher Scientific, Waltham, MA, USA). SEM-EDS analysis was performed on the JEOL JSM-6610LV instrument (JEOL Ltd., Tokyo, Japan). Before analysis, samples were coated with gold (the thickness of gold was 15 nm). Pore size distributions were determined by a high-pressure mercury intrusion porosimeter Carlo Erba Porosimeter 2000 (Washington, DC, USA, software Milestone 200). Nitrogen gas adsorption–desorption measurements were performed on a Sorptomatic 1990 Thermo Finnigan instrument at −196 °C (Thermo Fisher Scientific, Waltham, MA, USA). Elemental analysis (C, H, N) was performed on Perkin-Elmer Series II CHNS/O Analyzer 2400 (PerkinElmer, Inc., Waltham, MA, USA). Detection of aniline was determined by HPLC-MS (TSQ Quantum Access Max, Thermo Fisher Scientific, Waltham, MA, USA). Data were

acquired using Thermo Xcalibur software (version 3.0, Thermo Fisher Scientific, Waltham, MA, USA).

2.3. Synthesis of Core-Shell Amino-Functionalized MIP

2.3.1. Coating of Magnetite Nanoparticles with TEOS and MPS

The magnetite nanoparticles are coated with a two-stage process. The first step of coating with TEOS followed the procedure of Dil et al. [18], where 10 g magnetite nanoparticles were dispersed in a mixture of ethanol and water (4:1, *v*/*v*%) in an ultrasonic bath. Then, TEOS and NH_3 solution (1:2, *v*/*v*%) was added to the mixture and stirred for 8 h at 25 °C. Afterward, the obtained coated magnetite was washed with deionized water, dried in a vacuum at 60 °C for 24 h, and labeled as Fe_3O_4@SiO_2.

In the second step, Fe_3O_4@SiO_2 were dispersed in a mixture of ethanol–water (4:1, *v*/*v*%), then 40 mL of MPS was added, and the reaction mixture was left for 30 min in an ultrasonic bath. After that, NH_3 solution was added dropwise to the reaction mixture to adjust the pH to 5. The reaction was performed for 2 h at room temperature and 1 h at 50 °C under an inert nitrogen atmosphere. Finally, the sample was separated with a magnet, washed with ethanol, dried, and labeled as Fe_3O_4@SiO_2@MPS.

2.3.2. Synthesis of PGE60@Fe_3O_4@SiO_2@MPS Support

The magnetic polymer carrier was synthesized by the suspension copolymerization process. An aqueous phase (112.5 mL) (aqueous PVP solution, 7% by weight) was first added to the reaction flask and stirred for 30 min at 250 rpm. Thereafter, an organic phase consisting of a monomer (GMA (9.7 g), EGDMA cross-linker (6.47 g)), an initiator (AIBN (0.17 g)) and an inert component (cyclopentanol (16.9 g)) and tetradecanol (4.25 g)), previously dispersed with 1.6 g of Fe_3O_4@SiO_2@MPS, was added to the reactor for 30 min in an ultrasonic bath. The first 30 min reaction was performed at room temperature, then 2 h at 75 °C and 2 h at 80 °C at a stirring speed of 600 rpm. Finally, the polymer carrier was separated from the aqueous phase, washed with water and ethanol, dried in a vacuum, and labeled as PGE60@Fe_3O_4@SiO_2@MPS.

2.3.3. Synthesis of PEHA Functionalized MIP

MIP was synthesized by the surface imprinting method. In the first step, aniline and amine—PEHA were dissolved in 50 mL toluene and stirred for 2 h at 80 °C. Then, 2 g of PGE60@Fe_3O_4@SiO_2@MPS was added to the solution, and the reaction was performed for 6 h at 80 °C. The resulting sample was washed on Soxhlet with methanol–acetic acid (9:1) to wash the aniline and leave an imprint, dried in a vacuum at 60 °C, and labeled as MIP-PEHA.

2.4. Dispersive Solid-Phase Microextraction

First, 10 mL of water solution was transferred into a vial. The pH of the solution was adjusted to 6 by adding the appropriate amount of sodium hydroxide solution (0.1 M). At 25 °C, MIP-PEHA (50 mg) was added to the solution and stirred for 1 min under a vortex. The sorbent was separated by a strong magnet, and the supernatant was discharged. Then, acetonitrile (450 µL) was added to the sorbent. The mixture was stirred at 25 °C under a vortex for 1 min for aniline desorption. After the MIP was separated by a magnet, the acetonitrile phase was filtered and injected into HPLC-MS to analyze the aniline concentration. This procedure was successfully applied to determining aniline in the textile wastewater samples. The methodology flowchart is shown in Figure 2.

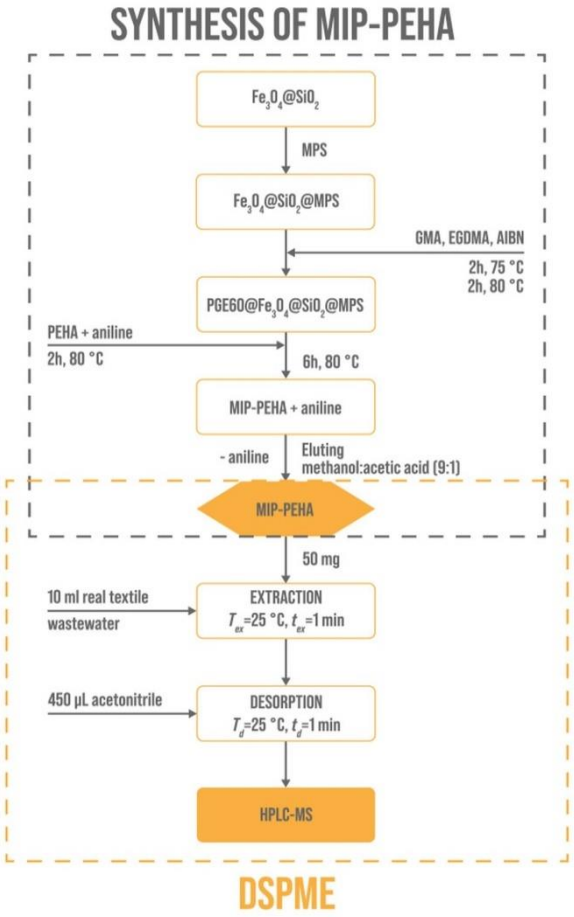

Figure 2. Methodology flowchart.

2.4.1. Plackett–Burman Design for the Screening of the Significant Variables

DoE combines mathematical and statistical methods to identify the significant variables and obtain optimum conditions [32]. PBD has been widely used to screen numerous variables with minimal effort. Advantages of PBD include simultaneous investigation of all variables instead of varying one variable with other constant conditions and information about two-way variables interactions, using a small number of experiments. PBD is equally helpful for any experiment which has many variables. It requires a smaller number of experiments compared to the full factorial design, and there is no need to limit the analysis to the most significant variables because all variables can be easily investigated [33].

In this study, PBD was created to screen the significant variables which affected the efficiency of DSPME. Each independent variable had two levels: −1 (low level) and +1 (high level) [34]. The variables and levels of the variables were considered based on the preliminary experiments and former publications: pH, extraction time, sorbent amount, ion strength, desorption time, and desorption volume are variables that were common to the literature [18,35–37].

Besides these variables, Dil et al. have taken into account vortex time, temperature, and centrifugation time. Due to magnetic properties and ease of removal of MIP-PEHA, centrifugation time was not taken into account [18]. Slavković-Beškoski et al. investigated the type of sorbent as a variable in the screening step [37]. In order to determine whether extraction and desorption are more efficient using ultrasound or vortex, this variable was also investigated. The range of variables was taken in the range of the above literature: sorbent mass (10–50 mg), ion strength (0–5 % w/v), desorption volume (100–700 µL), pH (3–11), temperature (10–40 °C), and vortex time (1–5 min).

The independent variables were dose of sorbent (m), pH, ionic strength (NaCl), vortex or ultrasonic extraction (U_{ex}), extraction time (t_{ex}), extraction temperature (T_{ex}), desorption

solvent volume (V_s), desorption temperature (T_d), vortex or ultrasonic desorption (U_d), desorption time (t_d), and type of eluent (*Solv*) (Table 1). In order to eliminate the effects of uncontrolled variables, experiments were randomly performed.

Table 1. Variables and levels of the PBD for the screening step.

Variables	Symbol	Level	
		Low	High
Dose of sorbent (mg)	m	10	50
pH	pH	2	10
Ionic strength (% w/v)	$NaCl$	0	1
Vortex or Ultrasonic extraction	U_{ex}	Vor	Us
Extraction time (min)	t_{ex}	1	5
Extraction temperature (°C)	T_{ex}	10	40
Desorption solvent volume (µL)	V_s	200	700
Desorption temperature (°C)	T_d	10	40
Vortex or Ultrasonic desorption	U_d	Vor	Us
Desorption time (min)	t_d	1	5
Type of eluent	$Solv$	Me	Ac

2.4.2. Optimization of Significant Variables by Box–Behnken Design

Box–Behnken design is used for further optimization of DSPME. This design is one of the most commonly used response surface methodologies. Compared to the three-level full factorial design and Central Composite Design (CCD), BBD showed more efficiency because it does not contain combinations where all variables are at their highest or lowest levels, thus avoiding extreme conditions, which can lead to unsatisfactory results [38].

In terms of efficiency, BBD has the advantage because of the relationship between the number of coefficients in the selected model and the number of experiments that need to be performed. V_s, pH, and T_{ex} were evaluated for further optimization in the ranges of 200–700 µL, 2–10, and 10–40 min, respectively. The main variables and their levels are shown in Table 2.

Table 2. Variables and levels of BBD for the optimization step.

Variables	Symbol	Level	
		Low	High
Desorption solvent volume (µL)	V_s	200	700
pH	pH	2	10
Extraction temperature (°C)	T_{ex}	10	40

Response surface methodology (RSM) is a set of experimental methods and statistical and mathematical approaches for developing a suitable correlation between a response parameter and the main variables and their interactions [39–42].

3. Results and Discussion

3.1. Characterization of Core-Shell Amino-Functionalized MIP

The obtained molecularly imprinted polymer was fully characterized, and the results are shown in Figures 3–6. The FTIR spectra of (a) Fe_3O_4@SiO_2, (b) Fe_3O_4@SiO_2@MPS, (c) PGE60@Fe_3O_4@SiO_2@MPS, and (d) MIP-PEHA are shown in Figure 3.

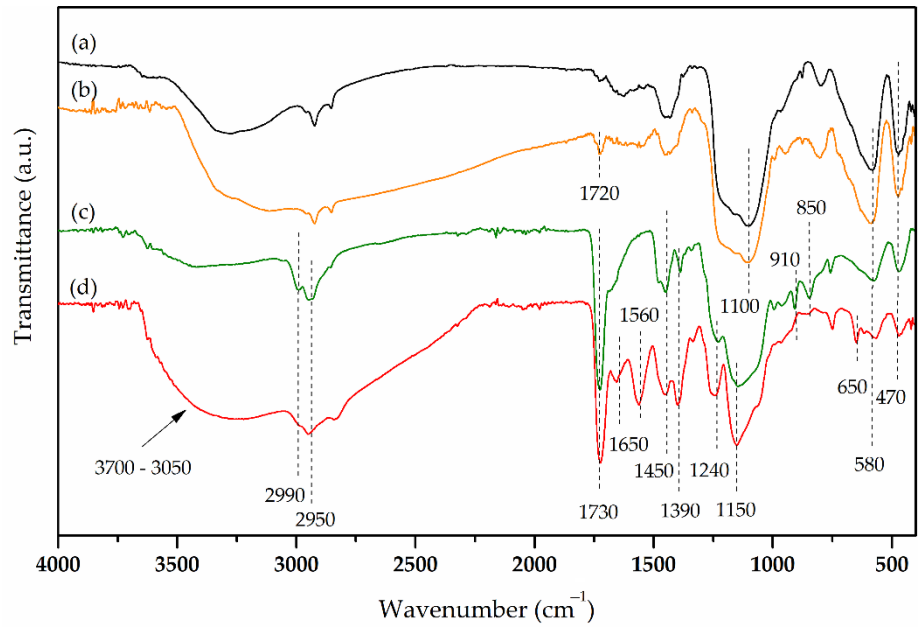

Figure 3. FTIR spectra of Fe_3O_4@SiO_2 (**a**), Fe_3O_4@SiO_2@MPS (**b**), PGE60@Fe_3O_4@SiO2@MPS (**c**), and MIP-PEHA (**d**).

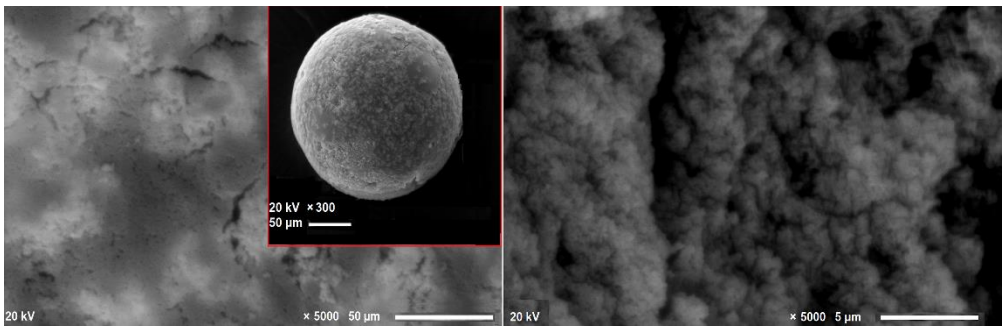

Figure 4. SEM micrographs of particle surface (**left**) and cross-section (**right**) for MIP-PEHA.

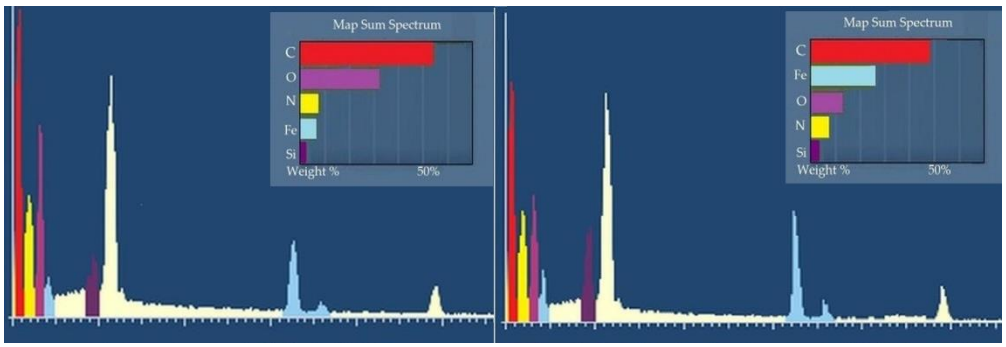

Figure 5. EDS of particle surface (**left**) and cross-section (**right**) of MIP-PEHA.

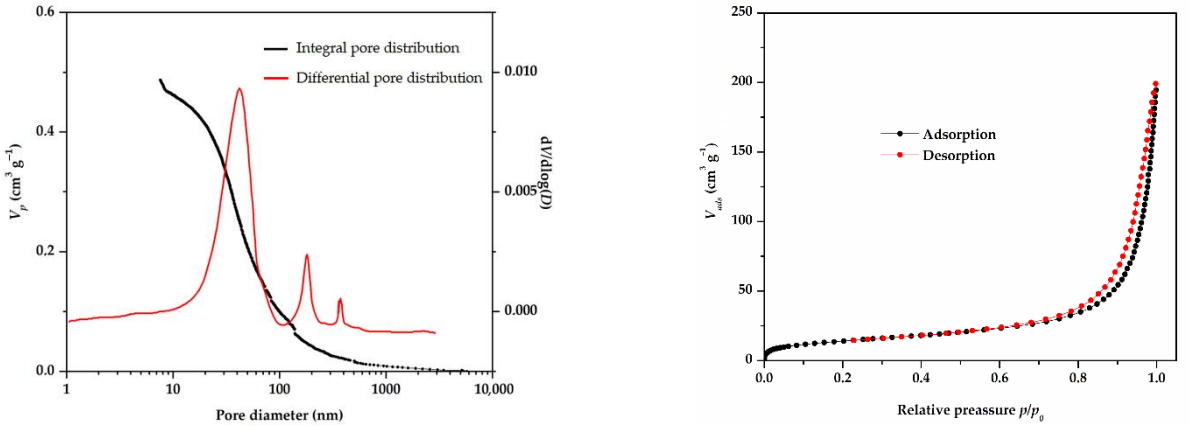

Figure 6. Cumulative and differential pore size distribution curves obtained by mercury porosimetry (**a**) and adsorption–desorption isotherms (**b**) for MIP-PEHA.

Fe–O stretching vibration is shown at 580 cm^{-1}. The peaks of Si–O–Si bending and asymmetric stretching vibration at 470 and 1100 cm^{-1}, respectively, confirm the formation of Fe_3O_4@SiO_2 (a). At 1721 cm^{-1} appears peak, which is associated with stretching vibration of C=O group of MPS (b) [43]. In the FTIR spectra of PGE60@Fe_3O_4@SiO_2@MPS, epoxy ring vibrations are observed at 850, 910, and 1260 cm^{-1} (νC-O). Additionally, a peak at ~1150 is assigned to C-O-C stretching vibration (νC-O-C).

The peaks at ~1470 and ~1390 cm^{-1} are related to symmetric and asymmetric methyl and methylene bending vibrations (δC-Hasym and δC-Hsym), while a strong band at ~1730 cm^{-1} suggests an ester carbonyl group (νC=O). The characteristic absorption bands at ~2990 cm^{-1} and 2950 cm^{-1} are attributed to methyl and methylene stretching vibrations (νC-H) [44]. In FTIR spectra of MIP-PEHA (d), peaks at ~1650 and ~1560 cm^{-1} originate from bending vibrations of N-H bonds (δN-H) of primary and secondary amines. In the wavelength area from 3700 to 3050 cm^{-1}, stretching vibrations of the N-H bonds (νN-H) of the primary and secondary amines and the O-H bond (νO-H) of the hydroxyl group overlap. At 650 cm^{-1} occurs N-H group wagging. The absence of epoxy bands in FTIR spectra of MIP-PEHA confirms the successful synthesis of MIP.

Scanning electron microscopy is used to observe particle surface and cross-section for MIP-PEHA (Figure 4). SEM micrograph (inserted picture in Figure 4) clearly shows a three-dimensional globular porous structure. EDS analysis of the sample-scanned area shows a relative proportion of all expected (C, O, N, Fe, and Si) both on the particle surface and on their cross-section (Figure 5).

The most abundant element with strong peaks is element C (53 wt.% for particle surface and 49 wt.% for cross-section). The N peaks confirm a successful amino-functionalization. Additionally, the percent of N for particle surface (7 wt.%) and cross-section (8 wt.%) indicated that the reaction of epoxy groups with the PEHA-aniline complex occurs equally on the particle surface as well as beneath the particle surface. Fe peaks (content for particle surface ~7 wt.%, and cross-section ~26 wt.%) indicate the incorporation of magnetite, while Si peaks (content for particle surface ~1 wt.%, and cross-section ~4 wt.%) show the silanization of magnetite particles. Stronger Fe and Si peaks on the cross-section suggest a core-shell structure of the sample particles. Moreover, the four-fold higher contents of the elements Fe and Si in the cross-section and almost three-fold higher content of element O in the particle surface indicate that the magnetite core is surrounded by a polymeric shell.

As shown in Figure 5, red peaks originate from carbon, pink peaks from oxygen, and blue and purple peaks determine the distribution of Fe and Si, respectively, while yellow peaks originate from N. The concentrations of C, H, and N calculated from the elemental analysis data were 50.9%, 6.9%, and 5.0%, respectively.

The porosity and pore size distribution were determined by mercury porosimetry. The results are shown in Figure 6a. Relevant porosity parameters of the sample calculated from the cumulative pore volume distribution curve were as follows: specific surface area, S_{Hg} = 60 m^2/g; specific pore volume, vs. = 0.487 $cm^3\ g^{-1}$, pore diameter, which corresponds to half of the pore volume, $d_{V/2}$ = 43 nm. The differential curve (red) determines the most dominant diameter, D_{max} = 45 nm. The cumulative curve has not reached the plateau, which indicates the presence of smaller mesopores and micropores that nitrogen gas adsorption-desorption measurements can better analyze at 77 K (Figure 6b).

According to the IUPAC classification, the curve corresponds to the Type II isotherm and H3 type of hysteresis loop [45]. The value of total pore volume ($V_{0.98}$) calculated according to the Gurvitch method for p/p_0 = 0.98 was 0.295 $cm^3\ g^{-1}$. The mesopores were analyzed using the Barrett, Joyner, Halenda method, while the micropores were analyzed by Dubinin–Radushkevich method, and their values were 0.24 $cm^3\ g^{-1}$ and 0.0147 $cm^3\ g^{-1}$, respectively. Based on both methods for analyzing the porous structure, it can be stated that the most dominant pores in the MIP-PEHA were mesopores.

3.2. Dispersive Solid-Phase Microextraction

Various variables can affect the extraction of the analytes by the DSPME technique. Moreover, these variables must be thoroughly considered and optimized to obtain the highest extraction efficiencies of the analytes. For this purpose, DoE was applied to reduce the number of experimental runs, cost, and experimentation time. This procedure includes a screening step followed by an optimization step.

3.2.1. MIP-DSPME Procedure Screening

The effects of the eleven selected variables were investigated in 12 runs. Variable effects are graphically analyzed using a Pareto chart, as shown in Figure 7. The Pareto chart is a simple graphical image of the effect of variables that simplifies the study of the effects of variables and their comparison on the responses. The results in the Pareto chart show the variables sorted by the impact on the response. The bar length is proportional to the significance of the variable for recovery (R%) of aniline. As seen, vs. is the most significant variable. Variables such as U_{ex}, NaCl, U_d, Solv are textual variables that have two levels that cannot be further optimized, so these variables are not taken for further optimization. The sorbent dose was fixed at a high level (an increment in the mass of the MIP-PEHA enhances the number of the active sites for efficient sorption of aniline), while t_{ex} and t_d were fixed at a low level. These variables had no significant effect on the R% of aniline in the studied range. Therefore V_s, pH, and T_{ex} were included for the next optimization step, while the fixed values of non-significant variables were 50 mg of sorbent, 1 min vortex extraction without salt addition, and 1 min vortex desorption at 25 °C with acetonitrile.

3.2.2. MIP-DSPME Procedure Optimization

After screening by the PBD, the predicted optimum conditions were obtained by the BBD. Therefore, a set of 15 experiments is designed to optimize the three selected variables from the screening step. The values were investigated in three levels: −1 (low level), 0 (center), and +1 (high level).

Once the ranges of relevant variables were selected, the response surface methodology, using BBD, was used to define the optimum conditions of significant variables. The response surface plots for aniline recovery are shown in Figure 8. The recovery reaches the highest levels when the temperature of extraction is 25 °C. This value did not require an additional investment of energy and made a cost-effective process. Aniline is stable under slightly acidic and neutral pH conditions, and by increasing the pH of the sample solution close to neutral pH, the R% of aniline was increased [46]. A pH value in the range of 2–10 was taken to avoid extreme conditions. The recovery showed the highest levels when the pH was 6.

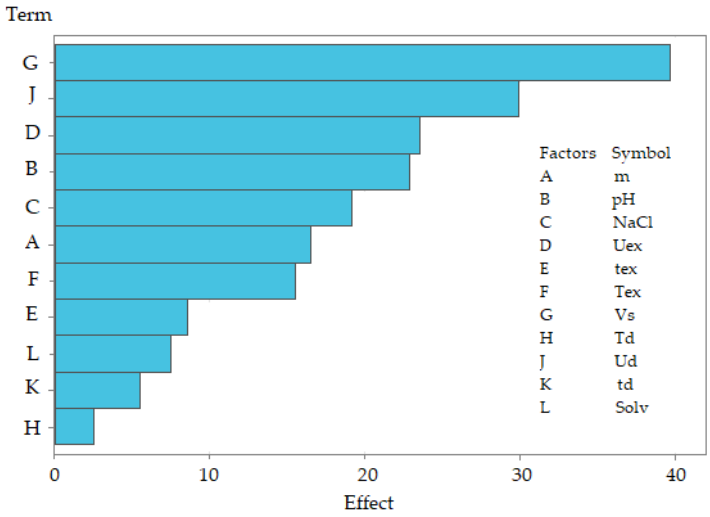

Figure 7. Pareto chart obtained from the screening step.

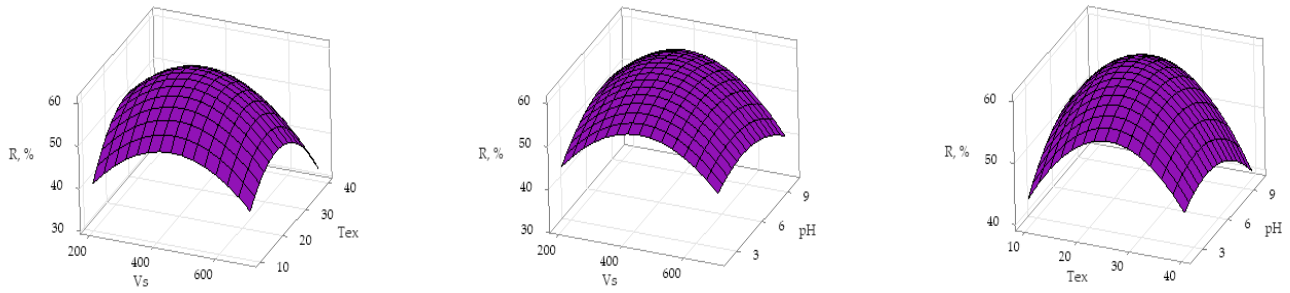

(**a**) (**b**) (**c**)

Figure 8. Response surface plots estimated by plotting extraction recovery (*R*%) versus: (**a**) *Tex* and vs. at *pH* 6; (**b**) *pH* and vs. at extraction temperature of 25 °C; and (**c**) *pH* and *Tex* at eluent volume of 450 µL.

Desorption solvent volume to elute a target analyte from a sorbent to achieve good recovery is one of the three most important variables in this research. Acetonitrile showed better R% than methanol for microextraction of aniline, and it was used for further optimization. The results are supported by the fact that the polarity of acetonitrile is closer to the aniline polarity (polarity order is methanol, acetonitrile, and aniline), and because of that, acetonitrile behaves as a better desorption solvent [47]. To investigate the impact of the desorption solvent volume on the R% of aniline, the range of 200–700 µL was analyzed. The recovery for aniline reaches the highest levels when the volume of AcN is 450 µL. At the same time, a minor decrease is observed with the eluent volumes above, which could be ascribed to the dilution effect of aniline in the eluent solution. As one of the most significant variables, the desorption volume of the solvent and pH is reported in the literature [12,35,36].

3.2.3. MIP-DSPME-HPLC method Validation

After the DSPME procedure is optimized, it is necessary to perform the validation procedure. Among the essential parameters for validation are the limit of detection (LoD), linearity, repeatability, and recovery. Experiments were performed at the optimum conditions explained in previous sections. According to the limit values, it is possible to define the lowest concentration of an aniline that can be reliably detected and quantified. The value of LoD was calculated from the signal, in which intensities are 3 times greater than the noise. The obtained value for LoD was 1 ng mL^{-1}. The calibration curves were constructed

by plotting the obtained peak areas of the analyte in the spiked aqueous solution with different concentrations in the range of 1–200 ng mL^{-1} after the extraction procedure under optimum conditions. The calibration curve for measuring aniline at different concentrations under optimal conditions was linear R-squared (R^2 = 0.9969). The calibration curve equation was calculated using the following equation: y = −1882 + 4270x. The repeatability was evaluated by determining the relative standard deviation (RSD) of the method for six replicates at a concentration of 10 ng mL^{-1} aniline in spiked aqueous solution. Application of DSPME to determine aniline in textile wastewater showed a recovery of 62% with an RSD of 18%.

3.3. Comparison to Other Methods

A comparison of the suggested DSPME-HPLC-MS method and other published methods used to detect aniline is presented in Table 3. It is seen that the method developed in this work displays equal or slightly lower LoD than one obtained for solid-phase microextraction followed by the gas chromatography-mass spectrometry method (SPME-GC-MS) [48], a single drop microextraction followed by the gas chromatography with flame-ionization detection (SDME-GC-FID) [49], headspace solid-phase microextraction coupled to gas chromatography-mass spectrometry (HS- SPME/GC-MS) [50], and solid-phase extraction followed by HPLC (SPE-HPLC) [51].

Table 3. Comparison with reported literature.

Methods	Extraction Phase	Linear Range (ng mL^{-1})	LoD (ng mL^{-1})	Total t_{ex} (min)	Reference
SPME-LC/MS-MS	Amphiphilic polymeric ionic liquid membrane	0.5–10	0.25	33	[52]
SPME-GC-MS	Poly(1-ethoxyethyl-3-(4-vinyl-phenyl)imidazolium chloride) fiber	0.05–10	4.29	40	[48]
SPE [a]-GC-FID	Poly(p-phenylenediamine)-Fe_3O_4 nanocomposite	0.03–100	0.007	2.5	[53]
SDME-GC-FID	Toluene	4–800	21	15	[49]
ITMA/HPLC-DAD [b]	poly(4-vinylbenzoic acid-*co*-dimethacrylate/divinylbenzene) monolith	0.1–300	0.026	21	[54]
HS-SPME/GC-MS	Polydimethylsioxane fibers	4.4–704	1.00	10	[50]
SPE-HPLC	Cigarette filter	0.025–10.0	5.46	7	[51]
HS-SPME/ GC-MS	Proton-type ionic liquid-doped polyaniline	0.195–100	0.024	42	[55]
DSPME-HPLC-MS	Amino-functionalized magnetic molecularly imprinted polymer based on glycidyl methacrylate	1–200	1.00	2	This study

[a] Solid-phase extraction. [b] In-tip microextraction apparatus followed by high-performance liquid chromatography with diode-array detection.

In addition, the total time of extraction (total t_{ex}) of aniline from water samples was a parameter used to illustrate the merits of the developed method further. The optimum total t_{ex} for DSPME is 2 min, which is less than the time needed for detecting aniline in other methods listed in Table 3. It was shown that the method applied in our work has a reasonably better or nearly the same LoD compared to others. The advantages of this research are reflected in the use of a small amount of sorbent, easy removal, low analysis time, and conditions that do not require an additional investment of energy in the process.

3.4. Determination of Aniline in Real Wastewater Samples

The suitability of the proposed DSPME technique for practical analysis was evaluated by the determination of aniline in real wastewater samples from different textile production facilities. To prepare the samples for the DSPME procedure, the samples were filtered through a Whatman 934-AH glass filter. All samples were determined by DSPME/HPLC-MS procedure under optimum conditions. Textile wastewater solution (10 mL) was transferred into a glass vial, and pH was adjusted to 6. Then, 50 mg of MIP-PEHA was added to the solution and stirred for 1 min under a vortex at 25 °C. After the supernatant was discharged and MIP-PEHA was separated with a strong magnet,

acetonitrile (450 µL) was added to the vial with sorbent. The solution was stirred under a vortex for 1 min at 25 °C. MIP-PEHA was separated with a magnet, and the acetonitrile phase was filtered and injected into HPLC-MS. Concentrations in real wastewater samples from three textile production facilities were obtained in the range of 6–300 ng mL^{-1}.

4. Conclusions

In this study, a core-shell magnetic molecularly imprinted polymer (MIP) based on glycidyl methacrylate (GMA) was successfully synthesized and functionalized with pentaethylenehexamine (PEHA). The silanized core of Fe_3O_4 nanoparticles enabled the magnetic properties of the polymer, suspension polymerization the production of spherical particles, and the surface imprinting method enabled an improved adsorption process. This approach to synthesizing MIPs was realized for the first time for the microextraction of aniline. FTIR and elemental analysis confirmed successful synthesis, mercury porosimetry, and nitrogen gas adsorption-desorption measurements have shown that the most dominant pores in the MIP-PEHA were mesopores ($Dmax$ = 45 nm), while SEM confirmed a 3D spherical porous structure. Synthetized MIP-PEHA was employed to extract aniline from textile wastewater. DSPME based on MIP-PEHA was optimized for preconcentration of aniline prior to HPLC-MS using DoE. PBD was used for the screening step to evaluate the significance of eleven variables at two levels, while BBD was applied to optimize the microextraction process. According to the Pareto chart, three variables (desorption solvent volume, pH, and extraction temperature) showed significant effects and were further optimized using BBD. The optimal conditions for successful microextraction of aniline were: 50 mg of sorbent, 1 min vortex extraction without salt addition at 25 °C, and 1 min vortex desorption at 25 °C with 450 µL of acetonitrile. These conditions proved to be cost-effective, time-saving, low solvent, and sorbent-consuming. The procedure exhibited acceptable linearity (R^2 = 0.9969), recovery ($R\%$ = 62), and limits of detection (LoD = 1 ng mL^{-1}). Aniline was detected in three real samples from textile production facilities in the range of 6–300 ng mL^{-1}. The results indicated that the proposed DSPME procedure is promising for aniline determination in textile wastewater.

Author Contributions: T.T.: investigation, writing—original draft preparation, software; B.M., formal analysis, data curation; J.R., validation, resources; J.L., methodology; L.S., visualization; A.N., conceptualization, project administration, funding acquisition; A.O., writing—review and editing, supervision. All authors have read and agreed to the published version of the manuscript.

Funding: This work was financially supported by the Ministry of Education, Science and Technological Development of the Republic of Serbia (Grant No. 451-03-68/2022-14/200026 and 451-03-68/2022-14/200135).

Institutional Review Board Statement: Not applicable.

Informed Consent Statement: Not applicable.

Data Availability Statement: The data presented in this study are available on request from the corresponding author.

Conflicts of Interest: The authors declare no conflict of interest.

References

1. Xue, G.; Wang, Q.; Qian, Y.; Gao, P.; Su, Y.; Liu, Z.; Chen, H.; Li, X.; Chen, J. Simultaneous Removal of Aniline, Antimony and Chromium by ZVI Coupled with H_2O_2: Implication for Textile Wastewater Treatment. *J. Hazard. Mater.* **2019**, *368*, 840–848. [CrossRef] [PubMed]
2. Ozmen, E.Y.; Sezgin, M.; Yilmaz, A.; Yilmaz, M. Synthesis of β-Cyclodextrin and Starch Based Polymers for Sorption of Azo Dyes from Aqueous Solutions. *Bioresour. Technol.* **2008**, *99*, 526–531. [CrossRef]
3. Tadrent, S.; Khelfa, A.; Len, C. Effect of KOH Pretreatment on Lignocellulosic Waste for the Reduction of Nitrobenzene to Aniline without Metal. *Sustainability* **2020**, *12*, 4665. [CrossRef]
4. Benkhaya, S.; M'rabet, S.; El Harfi, A. Classifications, Properties, Recent Synthesis and Applications of Azo Dyes. *Heliyon* **2020**, *6*, e03271. [CrossRef] [PubMed]

5. Trujillo-González, J.; Mahecha-Pulido, J.; Torres-Mora, M.; Brevik, E.; Keesstra, S.; Jiménez-Ballesta, R. Impact of Potentially Contaminated River Water on Agricultural Irrigated Soils in an Equatorial Climate. *Agriculture* **2017**, *7*, 52. [CrossRef]
6. Rubinos, D.A.; Spagnoli, G. Utilization of Waste Products as Alternative Landfill Liner and Cover Materials—A Critical Review. *Crit. Rev. Environ. Sci. Technol.* **2018**, *48*, 376–438. [CrossRef]
7. Egbueri, J.C.; Ukah, B.U.; Ubido, O.E.; Unigwe, C.O. A Chemometric Approach to Source Apportionment, Ecological and Health Risk Assessment of Heavy Metals in Industrial Soils from Southwestern Nigeria. *Int. J. Environ. Anal. Chem.* **2020**, *100*, 1–19. [CrossRef]
8. Xu, J.; Liu, Y.; Zhu, C.; Jia, H.; Tian, C.; Ma, H.; Lv, G. NaCl Improves Suaeda Salsa Aniline Tolerance in Wastewater. *Sustainability* **2020**, *12*, 7457. [CrossRef]
9. U.S.EPA. Integrated Risk Information System (IRIS) Chemical Assessment Summary (Aniline). Available online: https://iris.epa.gov/static/pdfs/0350_summary.pdf (accessed on 26 July 2022).
10. Habila, M.A.; Alhenaki, B.; El-Marghany, A.; Sheikh, M.; Ghfar, A.A.; ALOthman, Z.A.; Soylak, M. Metal Organic Framework-Based Dispersive Solid-Phase Microextraction of Carbaryl from Food and Water Prior to Detection by Ultra-Performance Liquid Chromatography-Tandem Mass Spectrometry. *Separations* **2022**, *9*, 32. [CrossRef]
11. Abughrin, S.E.; Alshana, U.; Bakirdere, S. Magnetic Nanoparticle-Based Dispersive Solid-Phase Microextraction of Three UV Blockers Prior to Their Determination by HPLC-DAD. *Int. J. Environ. Res. Public Health* **2022**, *19*, 6037. [CrossRef]
12. Ansari, S.; Masoum, S. A Multi-Walled Carbon Nanotube-Based Magnetic Molecularly Imprinted Polymer as a Highly Selective Sorbent for Ultrasonic-Assisted Dispersive Solid-Phase Microextraction of Sotalol in Biological Fluids. *Analyst* **2018**, *143*, 2862–2875. [CrossRef] [PubMed]
13. Ariani, M.D.; Zuhrotun, A.; Manesiotis, P.; Hasanah, A.N. Magnetic Molecularly Imprinted Polymers: An Update on Their Use in the Separation of Active Compounds from Natural Products. *Polymers* **2022**, *14*, 1389. [CrossRef] [PubMed]
14. Tolkou, A.K.; Kyzas, G.Z.; Katsoyiannis, I.A. Arsenic(III) and Arsenic(V) Removal from Water Sources by Molecularly Imprinted Polymers (MIPs): A Mini Review of Recent Developments. *Sustainability* **2022**, *14*, 5222. [CrossRef]
15. Kusumkar, V.V.; Galamboš, M.; Viglašová, E.; Daňo, M.; Šmelková, J. Ion-Imprinted Polymers: Synthesis, Characterization, and Adsorption of Radionuclides. *Materials* **2021**, *14*, 1083. [CrossRef] [PubMed]
16. Ansari, S. Application of Magnetic Molecularly Imprinted Polymer as a Versatile and Highly Selective Tool in Food and Environmental Analysis: Recent Developments and Trends. *TrAC Trends Anal. Chem.* **2017**, *90*, 89–106. [CrossRef]
17. Ali, G.K.; Omer, K.M. Molecular Imprinted Polymer Combined with Aptamer (MIP-Aptamer) as a Hybrid Dual Recognition Element for Bio(Chemical) Sensing Applications. Review. *Talanta* **2022**, *236*, 122878. [CrossRef]
18. Dil, E.A.; Doustimotlagh, A.H.; Javadian, H.; Asfaram, A.; Ghaedi, M. Nano-Sized FeO@SiO-Molecular Imprinted Polymer as a Sorbent for Dispersive Solid-Phase Microextraction of Melatonin in the Methanolic Extract of, Biological, and Water Samples. *Talanta* **2021**, *221*, 121620. [CrossRef]
19. Zengin, A.; Badak, M.U.; Aktas, N. Selective Separation and Determination of Quercetin from Red Wine by Molecularly Imprinted Nanoparticles Coupled with HPLC and Ultraviolet Detection. *J. Sep. Sci.* **2018**, *41*, 3459–3466. [CrossRef] [PubMed]
20. Tadić, T.; Marković, B.; Suručić, L.; Nastasović, A.; Onjia, A. Primena senzora na bazi molekulski otisnutih polimera za detekciju virusa. *Ecologica* **2021**, *28*, 543–550. [CrossRef]
21. Elmasry, M.R.; Tawfik, S.M.; Kattaev, N.; Lee, Y.-I. Ultrasensitive Detection and Removal of Carbamazepine in Wastewater Using UCNPs Functionalized with Thin-Shell MIPs. *Microchem. J.* **2021**, *170*, 106674. [CrossRef]
22. Sabri, M.A.; Sara, Z.; Al-Sayah, M.H.; Ibrahim, T.H.; Khamis, M.I.; El-Kadri, O.M. Simultaneous Adsorption and Reduction of Cr(VI) to Cr(III) in Aqueous Solution Using Nitrogen-Rich Aminal Linked Porous Organic Polymers. *Sustainability* **2021**, *13*, 923. [CrossRef]
23. Hasanah, A.N.; Safitri, N.; Zulfa, A.; Neli, N.; Rahayu, D. Factors Affecting Preparation of Molecularly Imprinted Polymer and Methods on Finding Template-Monomer Interaction as the Key of Selective Properties of the Materials. *Molecules* **2021**, *26*, 5612. [CrossRef] [PubMed]
24. Nastasović, A.; Marković, B.; Suručić, L.; Onjia, A. Methacrylate-Based Polymeric Sorbents for Recovery of Metals from Aqueous Solutions. *Metals* **2022**, *12*, 814. [CrossRef]
25. Suručić, L.; Tadić, T.; Janjić, G.; Marković, B.; Nastasović, A.; Onjia, A. Recovery of Vanadium (V) Oxyanions by a Magnetic Macroporous Copolymer Nanocomposite Sorbent. *Metals* **2021**, *11*, 1777. [CrossRef]
26. Sandić, Z.P.; Nastasović, A.B.; Jović-Jovičić, N.P.; Milutinović-Nikolić, A.D.; Jovanović, D.M. Sorption of Textile Dye from Aqueous Solution by Macroporous Amino-Functionalized Copolymer. *J. Appl. Polym. Sci.* **2011**, *121*, 234–242. [CrossRef]
27. Fontanals, N.; Marcé, R.M.; Borrull, F. Materials for Solid-Phase Extraction of Organic Compounds. *Separations* **2019**, *6*, 56. [CrossRef]
28. Li, H.; Hu, X.; Zhang, Y.; Shi, S.; Jiang, X.; Chen, X. High-Capacity Magnetic Hollow Porous Molecularly Imprinted Polymers for Specific Extraction of Protocatechuic Acid. *J. Chromatogr. A* **2015**, *1404*, 21–27. [CrossRef]
29. Parisi, O.I.; Cirillo, G.; Curcio, M.; Puoci, F.; Iemma, F.; Spizzirri, U.G.; Picci, N. Surface Modifications of Molecularly Imprinted Polymers for Improved Template Recognition in Water Media. *J. Polym. Res.* **2010**, *17*, 355–362. [CrossRef]
30. Ghosh, S.; Saha, S.; Sengupta, D.; Chattopadhyay, S.; De, G.; Basu, B. Stabilized Cu_2O Nanoparticles on Macroporous Polystyrene Resins [Cu_2O@ARF]: Improved and Reusable Heterogeneous Catalyst for On-Water Synthesis of Triazoles via Click Reaction. *Ind. Eng. Chem. Res.* **2017**, *56*, 11726–11733. [CrossRef]

31. Prabu, D.; Senthil Kumar, P.; Indraganti, S.; Sathish, S.; Aravind Kumar, J.; Vijai Anand, K. One-Step Fabrication of Amino-Functionalized Fe_3O_4@SiO_2 Core-Shell Magnetic Nanoparticles as a Potential Novel Platform for Removal of Cadmium (II) from Aqueous Solution. *Sustainability* **2022**, *14*, 2290. [CrossRef]
32. Egbosiuba, T.C.; Abdulkareem, A.S.; Tijani, J.O.; Ani, J.I.; Krikstolaityte, V.; Srinivasan, M.; Veksha, A.; Lisak, G. Taguchi Optimization Design of Diameter-Controlled Synthesis of Multi Walled Carbon Nanotubes for the Adsorption of Pb(II) and Ni(II) from Chemical Industry Wastewater. *Chemosphere* **2021**, *266*, 128937. [CrossRef] [PubMed]
33. Beres, D.L.; Hawkins, D.M. Plackett–Burman Technique for Sensitivity Analysis of Many-Parametered Models. *Ecol. Model.* **2001**, *141*, 171–183. [CrossRef]
34. Marrubini, G.; Dugheri, S.; Cappelli, G.; Arcangeli, G.; Mucci, N.; Appelblad, P.; Melzi, C.; Speltini, A. Experimental Designs for Solid-Phase Microextraction Method Development in Bioanalysis: A Review. *Anal. Chim. Acta* **2020**, *1119*, 77–100. [CrossRef]
35. Dozein, S.V.; Masrournia, M.; Es'haghi, Z.; Bozorgmehr, M.R. Development of a New Magnetic Dispersive Solid-Phase Microextraction Coupled with GC-MS for the Determination of Five Organophosphorus Pesticides from Vegetable Samples. *Food Anal. Methods* **2021**, *14*, 674–686. [CrossRef]
36. Sefaty, B.; Masrournia, M.; Es'haghi, Z.; Bozorgmehr, M.R. Determination of Tramadol and Fluoxetine in Biological and Water Samples by Magnetic Dispersive Solid-Phase Microextraction (MDSPME) with Gas Chromatography—Mass Spectrometry (GC-MS). *Anal. Lett.* **2021**, *54*, 884–902. [CrossRef]
37. Slavković-Beškoski, L.; Ignjatović, L.; Bolognesi, G.; Maksin, D.; Savić, A.; Vladisavljević, G.; Onjia, A. Dispersive Solid–Liquid Microextraction Based on the Poly(HDDA)/Graphene Sorbent Followed by ICP-MS for the Determination of Rare Earth Elements in Coal Fly Ash Leachate. *Metals* **2022**, *12*, 791. [CrossRef]
38. Ferreira, S.L.C.; Bruns, R.E.; Ferreira, H.S.; Matos, G.D.; David, J.M.; Brandao, G.C.; Souza, A.S. Box-Behnken Design: An Alternative for the Optimization of Analytical Methods. *Anal. Chim. Acta* **2007**, *597*, 179–186. [CrossRef] [PubMed]
39. Abdulrasheed, M.; Zulkharnain, A.; Zakaria, N.N.; Roslee, A.F.A.; Abdul Khalil, K.; Napis, S.; Convey, P.; Gomez-Fuentes, C.; Ahmad, S.A. Response Surface Methodology Optimization and Kinetics of Diesel Degradation by a Cold-Adapted Antarctic Bacterium, Arthrobacter Sp. Strain AQ5-05. *Sustainability* **2020**, *12*, 6966. [CrossRef]
40. Egbosiuba, T.C.; Abdulkareem, A.S.; Kovo, A.S.; Afolabi, E.A.; Tijani, J.O.; Roos, W.D. Enhanced Adsorption of As(V) and Mn(VII) from Industrial Wastewater Using Multi-Walled Carbon Nanotubes and Carboxylated Multi-Walled Carbon Nanotubes. *Chemosphere* **2020**, *254*, 126780. [CrossRef]
41. Vasiljević, T.; Onjia, A.; Čokeša, Đ.; Laušević, M. Optimization of Artificial Neural Network for Retention Modeling in High-Performance Liquid Chromatography. *Talanta* **2004**, *64*, 785–790. [CrossRef]
42. Lukić, J.; Radulović, J.; Lučić, M.; Đurkić, T.; Onjia, A. Chemometric Optimization of Solid-Phase Extraction Followed by Liquid Chromatography-Tandem Mass Spectrometry and Probabilistic Risk Assessment of Ultraviolet Filters in an Urban Recreational Lake. *Front. Environ. Sci.* **2022**, *10*, 916916. [CrossRef]
43. Javaheri, F.; Hassanajili, S. Synthesis of Fe_3O_4@SiO_2@MPS@P4VP Nanoparticles for Nitrate Removal from Aqueous Solutions. *J. Appl. Polym. Sci.* **2016**, *133*, 44330. [CrossRef]
44. Marković, B.M.; Vuković, Z.M.; Spasojević, V.V.; Kusigerski, V.B.; Pavlović, V.B.; Onjia, A.E.; Nastasović, A.B. Selective Magnetic GMA Based Potential Sorbents for Molybdenum and Rhenium Sorption. *J. Alloys Compd.* **2017**, *705*, 38–50. [CrossRef]
45. Thommes, M.; Kaneko, K.; Neimark, A.V.; Olivier, J.P.; Rodriguez-Reinoso, F.; Rouquerol, J.; Sing, K.S.W. Physisorption of Gases, with Special Reference to the Evaluation of Surface Area and Pore Size Distribution (IUPAC Technical Report). *Pure Appl. Chem.* **2015**, *87*, 1051–1069. [CrossRef]
46. Fakhri, A. Adsorption Characteristics of Graphene Oxide as a Solid Adsorbent for Aniline Removal from Aqueous Solutions: Kinetics, Thermodynamics and Mechanism Studies. *J. Saudi Chem. Soc.* **2017**, *21*, S52–S57. [CrossRef]
47. Vadukumpully, S. Carbon Nanofibers Extracted from Soot as a Sorbent for the Determination of Aromatic Amines from Wastewater Effluent Samples. *J. Chromatogr. A* **2011**, *1218*, 3581–3587. [CrossRef]
48. Zhang, Y.; Duan, Y. A Double-Functionalized Polymeric Ionic Liquid Used as Solid-Phase Microextraction Coating for Efficient Aromatic Amine Extraction and Detection with Gas Chromatography–Mass Spectrometry. *Anal. Bioanal. Chem.* **2019**, *411*, 2209–2221. [CrossRef]
49. Reddynoone, K.; Jain, A.; Verma, K. Liquid-Phase Microextraction and GC for the Determination of Primary, Secondary and Tertiary Aromatic Amines as Their Iodo-Derivatives. *Talanta* **2007**, *73*, 684–691. [CrossRef]
50. Chen, M.; Yin, Y.; Tai, C.; Zhang, Q.; Liu, J.; Hu, J.; Jiang, G. Analyses of Nitrobenzene, Benzene and Aniline in Environmental Water Samples by Headspace Solid Phase Microextraction Coupled with Gas Chromatography-Mass Spectrometry. *Chin. Sci. Bull.* **2006**, *51*, 1648–1651. [CrossRef]
51. Chen, S.; Liang, H.; Han, D. Determination of Aniline Derivatives in Water Samples by High Performance Liquid Chromatography Coupled with On-Line Flow Injection Preconcentration. *Anal. Lett.* **2010**, *43*, 2349–2355. [CrossRef]
52. Cai, M.-Q.; Wei, X.-Q.; Du, C.-H.; Ma, X.-M.; Jin, M.-C. Novel Amphiphilic Polymeric Ionic Liquid-Solid Phase Micro-Extraction Membrane for the Preconcentration of Aniline as Degradation Product of Azo Dye Orange G under Sonication by Liquid Chromatography–Tandem Mass Spectrometry. *J. Chromatogr. A* **2014**, *1349*, 24–29. [CrossRef]

53. Amiri, A.; Baghayeri, M.; Nori, S. Magnetic Solid-Phase Extraction Using Poly(Para-Phenylenediamine) Modified with Magnetic Nanoparticles as Adsorbent for Analysis of Monocyclic Aromatic Amines in Water and Urine Samples. *J. Chromatogr. A* **2015**, *1415*, 20–26. [CrossRef] [PubMed]
54. Wang, Z.; Liao, Y.; Chen, L.; Huang, X. On-Site Sample Preparation of Trace Aromatic Amines in Environmental Waters with Monolith-Based Multichannel in-Tip Microextraction Apparatus Followed by HPLC Determination. *Talanta* **2020**, *220*, 121423. [CrossRef] [PubMed]
55. Ai, Y.; Zhao, F.; Zeng, B. Novel Proton-Type Ionic Liquid Doped Polyaniline for the Headspace Solid-Phase Microextraction of Amines. *Anal. Chim. Acta* **2015**, *880*, 60–66. [CrossRef] [PubMed]